

SCIENTIFIC REPORTS

OPEN

Perfluorooctanesulfonate (PFOS)-induced Sertoli cell injury through a disruption of F-actin and microtubule organization is mediated by Akt1/2

Ying Gao¹, Haiqi Chen¹, Xiang Xiao^{1,2}, Wing-yei Lui³, Will M. Lee³, Dolores D. Mruk¹ & C. Yan Cheng¹ 

PFOS (perfluorooctanesulfonate, or perfluorooctane sulfonic acid) is an anthropogenic fluorosurfactant widely used in consumer products. While its use in Europe, Canada and the U.S. has been banned due to its human toxicity, it continues to be used in China and other developing countries as a global pollutant. Herein, using an *in vitro* model of Sertoli cell blood-testis barrier (BTB), PFOS was found to induce Sertoli cell injury by perturbing actin cytoskeleton through changes in the spatial expression of actin regulatory proteins. Specifically, PFOS caused mis-localization of Arp3 (actin-related protein 3, a branched actin polymerization protein) and palladin (an actin bundling protein). These disruptive changes thus led to a dis-organization of F-actin across Sertoli cell cytosol, causing truncation of actin microfilament, thereby failing to support the Sertoli cell morphology and adhesion protein complexes (e.g., occludin-ZO-1, CAR-ZO-1, and N-cadherin- β -catenin), through a down-regulation of p-Akt1-S473 and p-Akt2-S474. The use of SC79, an Akt1/2 activator, was found to block the PFOS-induced Sertoli cell injury by rescuing the PFOS-induced F-actin dis-organization. These findings thus illustrate PFOS exerts its disruptive effects on Sertoli cell function downstream through Akt1/2. As such, PFOS-induced male reproductive dysfunction can possibly be managed through an intervention on Akt1/2 expression.

PFOS is a global pollutant and an environmental toxicant, widely used as a fabric protector, serving as a stain repellant in drapery, carpets and clothing. Its use in consumer products has been discontinued and banned in Europe, Canada and the U.S. since the 2000s due to its health risks associated with human, wildlife and animal exposure including reduced fetal growth, endocrine disruption, reproductive dysfunction, and neonatal mortality^{1–4}. However, epidemiologic evidence does not support a causal association between PFOS exposure and cancer risk in humans⁵. Nonetheless, in utero exposure to PFOS adversely affect the fetal synthesis and secretion of reproductive hormones (e.g., testosterone, estradiol, and inhibin B) in humans⁶. Since the half-life of PFOS and its related compound PFOA (perfluorooctanoic acid) is relatively long, at 5.4-yr and 3.8-yr, respectively^{7,8}, even low-dose exposure to PFOS and its related compounds can accumulate in the body over an extended period of time. At present, studies in rodents have generally supported the notion that PFOS perturbs testis function, such as by inducing Sertoli cell injury and disrupting Leydig cell steroidogenic function^{9–12}. A recent study from our laboratory has shown that the PFOS-mediated Sertoli cell injury that impedes blood-testis barrier (BTB) function using an *in vitro* model of primary Sertoli cells is through a disruption of actin-based cytoskeleton in Sertoli cells, involving p-FAK-Y407¹³, which is an activated form of FAK earlier shown to be involved in BTB remodeling during spermatogenesis¹⁴. The notion that FAK is involved in PFOS-mediated Sertoli cell injury was

¹The Mary M. Wohlford Laboratory for Male Contraceptive Research, Center for Biomedical Research, Population Council, 1230 York Ave, New York, New York, 10065, USA. ²Department of Reproductive Physiology, Zhejiang Academy of Medical Sciences, Hangzhou, 310013, China. ³School of Biological Sciences, The University of Hong Kong, Pokfulam, Hong Kong, China. Ying Gao and Haiqi Chen contributed equally to this work. Correspondence and requests for materials should be addressed to C.Y.C. (email: Y-Cheng@popcbr.rockefeller.edu) or X.X. (email: xxiao@zjams.com) or W.Y.L. (email: wylui@hku.hk)

further confirmed by using an endogenous miRNA specific for FAK, miR-135b, which was found to perturb the Sertoli TJ-permeability barrier alone, and also worsened PFOS-induced TJ-barrier disruption¹³. However, over-expression of a constitutive active phosphomimetic mutant of p-FAK-Y407, namely p-FAK-Y407E, by mutating Tyr(Y)-407 to Glu(E)-407, in Sertoli cells could protect these cells from the damaging effects of PFOS¹³.

Recent studies have shown that the Sertoli cell BTB function is mediated by mTORC1 complex through rpS6, involving Akt1/2 downstream, which in turn modulates F-actin organization in Sertoli cells¹⁵, but also involving MMP9 activation¹⁶. Other studies also support the involvement of FAK in mTOR signaling¹⁷, and the involvement of MMP2 and FAK in Akt signaling¹⁸. In order to better understand the signaling pathway of FAK-mediated rescue function during PFOS-induced Sertoli cell injury, we sought to examine the involvement of Akt in PFOS-mediated Sertoli cell injury, and its functional relationship with p-FAK-Y407. This mechanistic study thus provides additional insight on the molecular mechanism by which PFOS causes reproductive dysfunction in males through its disruptive effects on the Sertoli cell of the mammalian testis.

Results

PFOS perturbs TJ- and basal ES-protein localization in Sertoli cells – an involvement of p-Akt1/2?

Sertoli cells isolated from 20-day-old rat testes were cultured *in vitro* for 3 days to form a cell epithelium with an established functional TJ-barrier, which mimicked the Sertoli cell BTB *in vivo*^{19–22}. This *in vitro*-based system has been widely used by investigators to study BTB dynamics^{23–29}, and many of the findings were subsequently confirmed by studies *in vivo*^{30–33}. Thereafter, these cells were treated with PFOS at 10, 20 or 50 μ M for 24 hr. It was noted that PFOS perturbed the Sertoli cell TJ-permeability barrier function dose-dependently with PFOS at 50 μ M was more effectively to perturb the TJ function than at 20 μ M (Fig. 1A). The range of PFOS concentration at 20–50 μ M (i.e., at ~10–25 μ g/ml) used in our study herein was shown not to be cytotoxic as recently reported from our laboratory, and no cytotoxicity was found at concentration up to 100 μ M¹³. At present the acceptable daily intake (ADI) of PFOS is 150 ng/kg/day (for a review, see ref. 34). But since PFOS has a human elimination half-life of 5.4-year^{7,8}, a considerable level of PFOS could build up in humans in particular among industrial workers such as those who utilize PFOS for manufacturing of stain resistant carpets and fabrics.

Lysates from Sertoli cells at specified time points were then obtained for immunoblotting using corresponding specific antibodies which were characterized earlier in our laboratory (Table 1)^{35,36}. The steady-state levels of TJ-proteins occludin and CAR, and basal ES-proteins N-cadherin and β -catenin, branched actin polymerization protein Arp3, barbed end capping and bundling protein Eps8, and actin nucleation protein formin 1 were not perturbed following PFOS treatment, but TJ-adaptor protein ZO-1 and actin bundling proteins palladin and plastin 3 were down-regulated (Fig. 1B; Figure S1A). More important, considerable down-regulation of p-Akt1-T308, p-Akt1-S473, and p-Akt2-S474 were noted, but not total Akts including 1–3 (Fig. 1B; Figure S1A). The down-regulation of p-FAK-Y407, but not total FAK, was also noted (Fig. 1B), consistent with an earlier report¹³. We also detected no changes in the expression EB1 (a plus (+)-end tracking protein, +TIP, of MT, known to stabilize MT³⁷) but a down-regulation on the expression of dephosphorylated α -tubulin (i.e., removal of C-terminal Tyr by exposing Glu as the N-terminal residue known to stabilize MT, making MT less dynamic³⁸). Gross mis-localization of TJ proteins occludin, CAR and ZO-1, as well as basal ES proteins N-cadherin and β -catenin at the Sertoli cell-cell interface was also noted wherein these proteins no longer tightly associated with the cell cortical zone, but internalized and moved into the cell cytosol (Fig. 1C; Figure S1B). These changes thus de-stabilized the Sertoli cell barrier function.

PFOS perturbs Sertoli cell TJ-barrier function through changes in the spatial expression of actin binding and regulatory proteins.

Since the TJ- and basal ES-proteins that displayed mis-localization at the Sertoli cell-cell interface noted in Fig. 1C all utilized F-actin for attachment, we next examined any changes in the F-actin organization in Sertoli cells following PFOS treatment. As expected, F-actin organization was grossly affected by PFOS treatment in which long stretches of actin microfilaments no longer laid across the Sertoli cell cytosol in an organized fashion as noted in control cells (left column), they became truncated, and in some cells they were also branched in two different experiments shown in the middle and right columns (Fig. 2). These changes in actin organization appeared to be the result of changes in spatial localization of branched actin polymerization protein Arp3 and actin bundling protein palladin which confer actin microfilaments into a bundled configuration, leading to actin filament bundles into a disorganized branched network. For instance, Arp3 no longer localized mostly at the cell-cell interface, but re-localized and moved into the cell cytosol (Fig. 2). Palladin also no longer stretched across the Sertoli cell cytosol to organize actin filaments into bundles as seen in controls, instead, palladin retracted from cell cytosol and found closer to the cell nuclei following PFOS treatment (Fig. 2). p-FAK-Y407, a known TJ regulator in the testis¹⁴ also considerably mis-localized in which they no longer found at the Sertoli cell-cell interface, but all diffusely localized in the cell cytosol (Fig. 2).

Rescue of PFOS-induced Sertoli cell TJ-barrier disruption by SC79, an activator of Akts through changes in the re-distribution of BTB-associated proteins.

Recent studies have shown that Sertoli cell TJ-barrier disruption is mediated downstream via Akt1/2 through a down-regulation of p-Akt1-S473 and p-Akt2-S474¹⁵. We speculated an induction of p-Akt1/2 via the use of a membrane permeable Akt phosphorylation activator SC79³⁹ might prevent the PFOS-mediated Sertoli cell TJ-permeability disruption, and might also rescue the PFOS-induced mis-localization of TJ- and basal ES-proteins at the Sertoli cell-cell interface. Indeed, the use of SC79 was found to block the PFOS-induced down-regulation of ZO-1, palladin, p-Akt1-T308 and p-Akt1-S473 (but not p-Akt2-S474) (Fig. 3A; Figure S2A). It is of interest to note that SC79 itself activated p-Akt1-T308 and p-Akt1-S473 in DMSO-vehicle control group (Fig. 3A lane 1 vs. lane 3). However, SC79 *per se* had no apparent effects on the Sertoli cell TJ-permeability barrier function (Fig. 3B). But SC79 blocked the PFOS-induced Sertoli cell TJ barrier disruption when the barrier function was monitored across the Sertoli cell

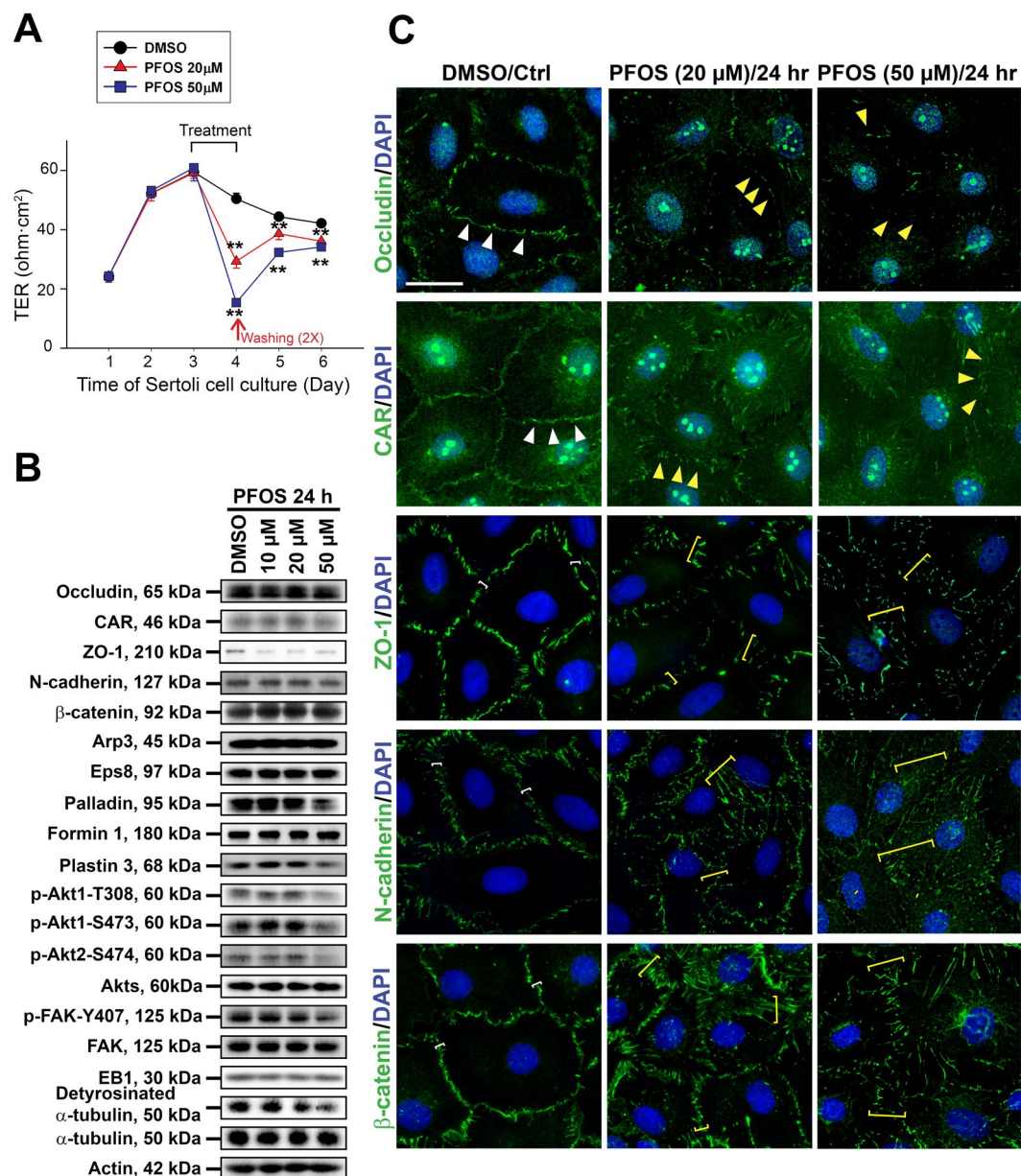


Figure 1. PFOS perturbs Sertoli cell BTB function through changes in the expression and/or localization of proteins at the immunological barrier. Sertoli cells cultured on Matrigel-coated bicameral units, dishes or coverslips were treated on day 3 with 10, 20 or 50 μM PFOS for 24 hr. Thereafter, cells were washed twice with PBS to remove residual PFOS and terminated for immunoblotting (IB) or IF on day 4. **(A)** Typical results of a TER experiment that monitored the effects of PFOS, at 20 μM and 50 μM vs. vehicle control (DMSO) on the Sertoli cell TJ-permeability barrier. Each data point is a mean ± SD of triplicate units from an experiment, which was repeated 3 times and yielded similar results. $^{**}P < 0.01$ by Student's *t*-test compared between PFOS-treated and control cells. **(B)** Immunoblot analysis to assess the effects of PFOS on the expression of TJ proteins: occludin, CAR and ZO-1; basal ES proteins: N-cadherin and β-catenin; actin regulatory proteins: Arp3, Eps8, palladin, formin 1 and plastin 3; signaling molecules: activated Akts: p-Akt1-T308, p-Akt1-S473, p-Akt2-S474 vs. Akts (including Akt1, 2 and 3), and activated FAK: p-FAK-Tyr407 vs. FAK; MT regulatory proteins: EB1 and detyrosinated α-tubulin. Actin and α-tubulin served as protein loading controls. PFOS was found to down-regulate p-Akt1-T308, p-Akt1-S473, p-Akt2-S474 and p-FAK-Tyr407. Composite data of immunoblottings are shown in Figure S1A; and uncropped blots are shown in Figure S4. **(C)** Immunofluorescence analysis to assess the effects of PFOS at 20 μM and 50 μM vs. control on the distribution of TJ proteins: occludin, CAR and ZO-1; basal ES proteins: N-cadherin and β-catenin. PFOS caused internalization of TJ and basal ES proteins in Sertoli cells in which these proteins no longer tightly localized at the Sertoli cell-cell interface. Occludin and CAR at the cell-cell interface (annotated by white arrowheads) were diminished following PFOS treatment (yellow arrowheads). For ZO-1, N-cadherin and β-catenin, these proteins were localized tightly at the cell-cell interface (white brackets) but were considerably internalized, diffusing away from the cell cortical zone (yellow brackets). Sertoli cell nuclei were visualized by DAPI. Composite analyzed data are shown in Figure S1B. Scale bar, 30 μm.

Antibody	Host species	Vendor	Catalog no.	Working dilution	
				IB	IF/IHC
Actin	Goat	Santa Cruz Biotechnology	sc-1616	1:300	
Arp3	Mouse	Sigma-Aldrich	A5979	1:3000	1:50
Akt	Rabbit	Cell Signaling Technology	9272	1:1000	
p-Akt T308	Rabbit	Cell Signaling Technology	2965	1:1000	
p-Akt1 S473	Rabbit	Cell Signaling Technology	4060	1:1000	
p-Akt2 S474	Rabbit	Cell Signaling Technology	8599	1:1000	
α -tubulin	Mouse	Abcam	ab7291		1:500 (tissue) 1:300 (cell)
β -catenin	Rabbit	Thermo Fisher Scientific	71–2700	1:2000	1:100
CAR	Rabbit	Santa Cruz Biotechnology	sc-15405	1:200	1:50
Detyrosinated α -tubulin	Rabbit	Abcam	ab48389	1:1000	1:200
EB1	Mouse	BD Biosciences	610534		1:200
EB1	Rabbit	Santa Cruz Biotechnology	sc-15347	1:200	
Eps8	Mouse	BD Biosciences	610143	1:5000	1:50
Formin 1	Mouse	Abcam	ab68058	1:500	1:50
FAK	Mouse	Millipore	05–537	1:1000	
p-FAK-Tyr407	Rabbit	Thermo Fisher Scientific	44–650G	1:1000	1:50
N-cadherin	Mouse	Thermo Fisher Scientific	33–3900	1:200	1:100
Ocludin	Rabbit	Thermo Fisher Scientific	71–1500	1:250	1:100
Palladin	Rabbit	Proteintech	10853–1-AP	1:1000	1:100
Plastin 3	Rabbit	Abcam	ab137585	1:500	
ZO-1	Rabbit	Thermo Fisher Scientific	61–7300	1:250	1:100
Goat IgG-HRP	Bovine	Santa Cruz Biotechnology	sc-2350	1:3000	
Rabbit IgG-HRP	Bovine	Santa Cruz Biotechnology	sc-2370	1:3000	
Mouse IgG-HRP	Bovine	Santa Cruz Biotechnology	sc-2371	1:3000	
Rabbit IgG-Alexa Fluor 488	Goat	Thermo Fisher Scientific	A-11034		1:250
Mouse IgG-Alexa Fluor 488	Goat	Thermo Fisher Scientific	A-11029		1:250

Table 1. Antibodies used for different experiments in this study. Abcam, Cambridge, MA; Cell Signaling Technology, Danvers, MA; Santa Cruz Biotechnology, Santa Cruz, CA; Sigma-Aldrich, St. Louis, MO; Invitrogen, Life Technologies, Carlsbad, CA; Proteintech, Chicago, IL; BD Biosciences, San Jose, CA; Millipore Corp., Billerica, MA.

epithelium on Matrigel-coated bicameral units (Fig. 3B). The ability of SC79 to rescue Sertoli cells from the disruptive effects of PFOS onto the TJ-barrier function was mediated through changes in the re-distribution of TJ-proteins CAR and ZO-1, as well as basal ES-proteins N-cadherin and β -catenin since SC79 treatment managed to re-localize these BTB-associated proteins back to the Sertoli cell-cell interface compared to PFOS-treated cells without SC79 pre-treatment (Fig. 3C; Figure S2B). These findings thus support the notion that PFOS exerts its disruptive effects on the Sertoli cell-TJ barrier function via p-Akt signaling protein involving p-Akt1-T308 and p-Akt1-S473 but not p-Akt2-S474. Furthermore, this disruptive effect can be blocked via the use of an Akt activator SC79.

Rescue of PFOS-induced Sertoli cell TJ-barrier disruption by SC79 through changes in the organization of actin-based cytoskeleton. We next examined the underlying molecular mechanism by which SC79, the activator of Akt, blocked the PFOS-mediated disruption on the Sertoli cell TJ-permeability barrier and by re-distributing BTB-associated proteins at the Sertoli cell-cell interface as noted in Fig. 3. As shown in Fig. 4 (top left panel), treatment of Sertoli cells with PFOS induced disorganization of actin microfilaments in Sertoli cells through changes in the spatial expression of Arp3, palladin and p-FAK-Y407 (a BTB regulator that confers BTB integrity) (Fig. 4, left panels). For instance, actin microfilaments across the Sertoli cell cytosol became truncated, no longer orderly organized and that stretched across the cell cytosol as found in control cells treated with DMSO alone (Fig. 4). The orderly alignment of actin microfilaments found in control cells were likely the result of spatial expression of Arp3 and p-FAK-Y407, mostly at the cell-cell interface and also palladin which conferred actin microfilaments their bundled configuration as noted in control cells (Fig. 4). Following PFOS treatment, Arp3 no longer localized prominently at the cell-cell interface but internalized, similar to p-FAK-Y407 (see Figure S3), and palladin appeared to be retracted from the cell cytosol but localized closely to the cell nucleus (Fig. 4). However, treatment of SC79 prevented PFOS-induced changes in the spatial expression of Arp3 wherein this branched actin polymerization protein became localized more prominent at the Sertoli cell-cell interface, similar to control, instead of rapidly internalized as noted in PFOS-treated Sertoli cells (Fig. 4, Figure S3). This pattern of changes was similar to p-FAK-Y407 (Fig. 4, Figure S3). Furthermore, palladin was also found to stretch across the entire Sertoli cell cytosol in SC79 treated cells, blocking the PFOS-induced disruption of palladin

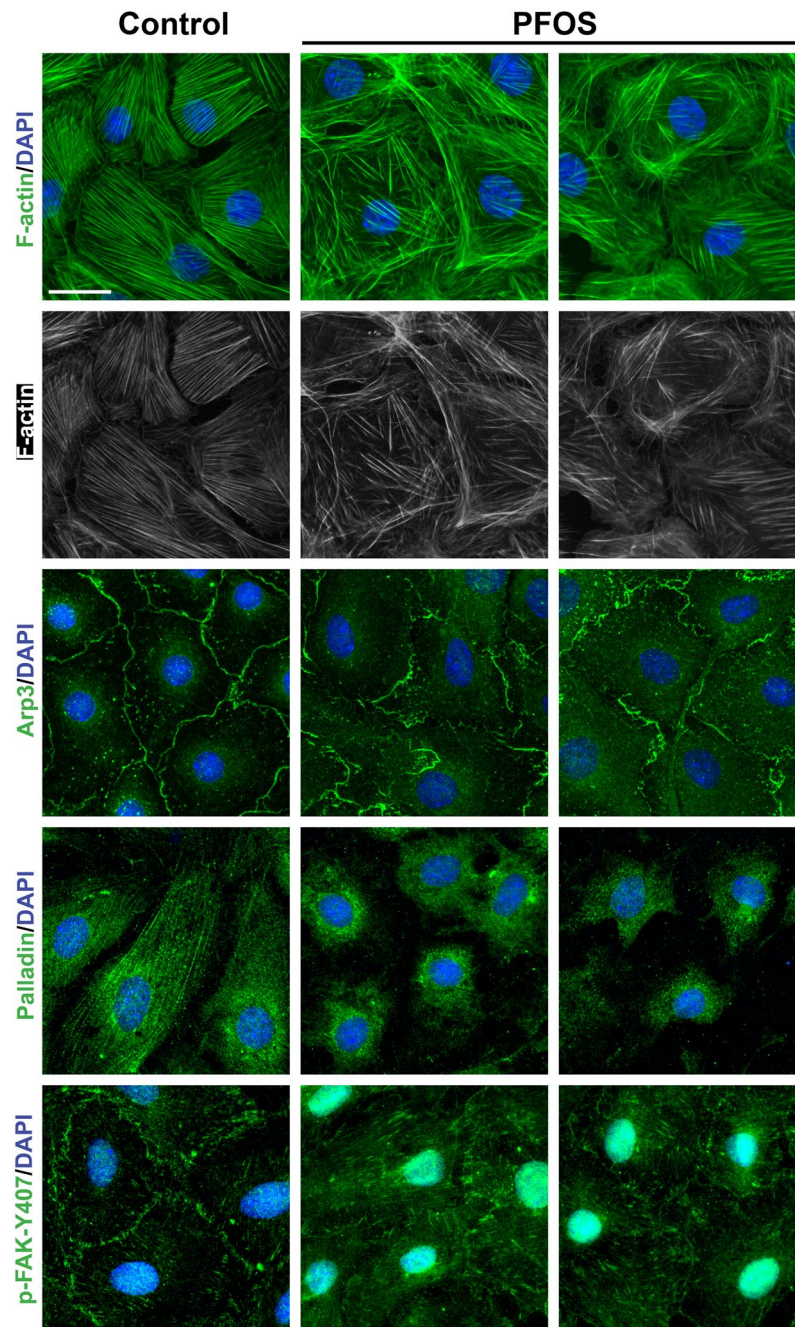


Figure 2. Immunofluorescence analysis to assess the effects of PFOS on the organization of actin microfilaments in Sertoli cells via changes on the distribution of actin regulatory proteins. Sertoli cells cultured for 3 days were treated with 20 μ M PFOS for 24 hr. Cells were then harvested and used for IF, and results from two different experiments were shown in middle and right columns vs. the control cells in the left column. PFOS caused truncation and defragmentation of F-actin network (green and gray). These changes in the organization of actin microfilaments were likely the result of changes in the spatial localization of several actin regulatory proteins. Arp3, a branched actin polymerization protein that effectively converted actin microfilaments into a branched/unbundled configuration no longer localized at the cell-cell interface to support F-actin dynamics at the cell cortical zone. Instead, Arp3 was internalized and found in the Sertoli cell cytosol, thereby impeding actin microfilaments to organize as long actin bundles stretched across the cell cytosol. Palladin, an actin cross-linking and bundling protein, no longer stretched across the Sertoli cell cytosol to maintain actin microfilaments across the Sertoli cells as found in control cells. Instead, palladin was retracted from the cell peripheries but concentrated to cell nuclei after PFOS treatment. p-FAK-Y407, a signaling protein shown to be involved in maintaining BTB integrity by maintaining F-actin network in Sertoli cells as actin filament bundles also no longer localized to the Sertoli cell-cell interface to maintain the TJ-barrier function. Instead, it was internalized into the cell cytosol, thereby destabilizing the TJ-barrier function. Sertoli cell nuclei were visualized by DAPI. Scale bar, 30 μ m.

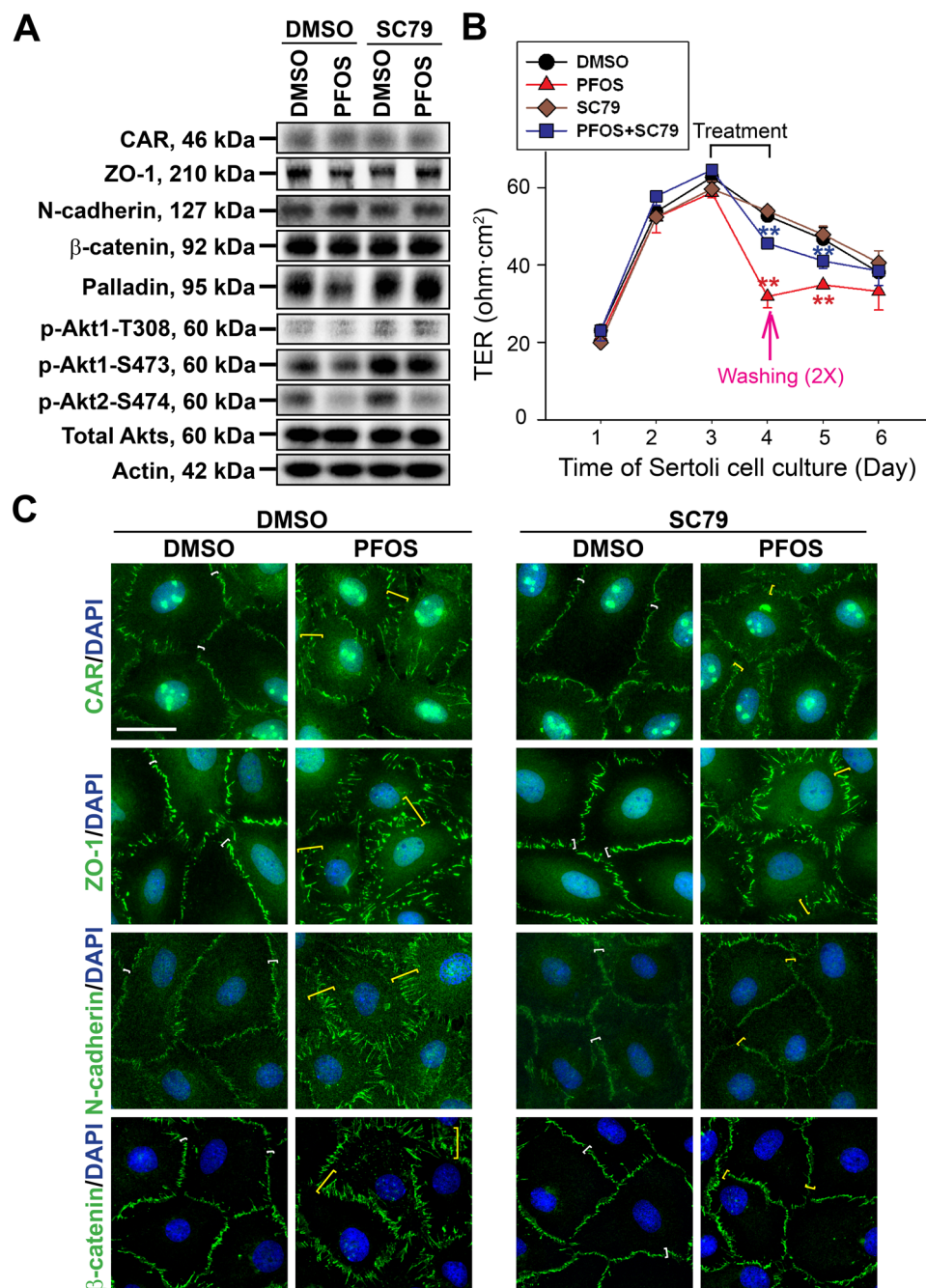


Figure 3. Akt activator SC79 blocks PFOS-mediated Sertoli cell TJ-barrier disruption and mis-localization of TJ and basal ES proteins at the BTB. (A) Sertoli cells cultured at 0.1×10^6 cells/cm² (in 6-well dishes with 2 ml F12/DMEM per well) for 3 days were pre-treated with SC79 at 2 μ g/ml (5.5 μ M) for 30 min. Cells were rinsed and treated with 50 μ M PFOS for 24 hr for immunoblotting. SC79 was found to up-regulate the PFOS-induced down-regulation of p-Akt1 T308 and p-Akt1 S473, but had no apparent effect in blocking the PFOS-induced down regulation of p-Akt2 S474. SC79 was also found to rescue PFOS-induced down-regulation on the expression of ZO-1, palladin. Actin served as a loading control. Composite analyzed data of immunoblottings are shown in Figure S2A; and uncropped blots are shown in Figure S5. (B) A study by TER to assess the ability of SC79 to block the PFOS-mediated disruption of the Sertoli cell TJ-permeability barrier function. Treatment of PFOS alone perturbed the TJ-barrier function, $**P < 0.01$, by Student's *t*-test compared between PFOS treated cells vs. control (DMSO) cells; $**P < 0.01$, by Student's *t*-test compared between PFOS + SC79-treated cells vs. PFOS-treated cells. (C) Sertoli cells cultured at 0.04×10^6 cells/cm² for 3 days were pre-treated with 2 μ g/ml SC79 for 30 min, and then cells were rinsed and treated with 20 μ M PFOS for 24 hr. Thereafter, cells were then fixed and examined by immunofluorescence microscopy. SC79 treatment was found to block PFOS-induced mis-localization of TJ proteins CAR and ZO-1, as well as basal ES proteins N-cadherin and β -catenin. BTB-associated proteins at the Sertoli cell-cell interface in control and PFOS-treated cells were annotated by corresponding white and yellow brackets, respectively. Composite analyzed data of this experiment are shown in Figure S2B. Sertoli cell nuclei were visualized by DAPI. Scale bar, 30 μ m.

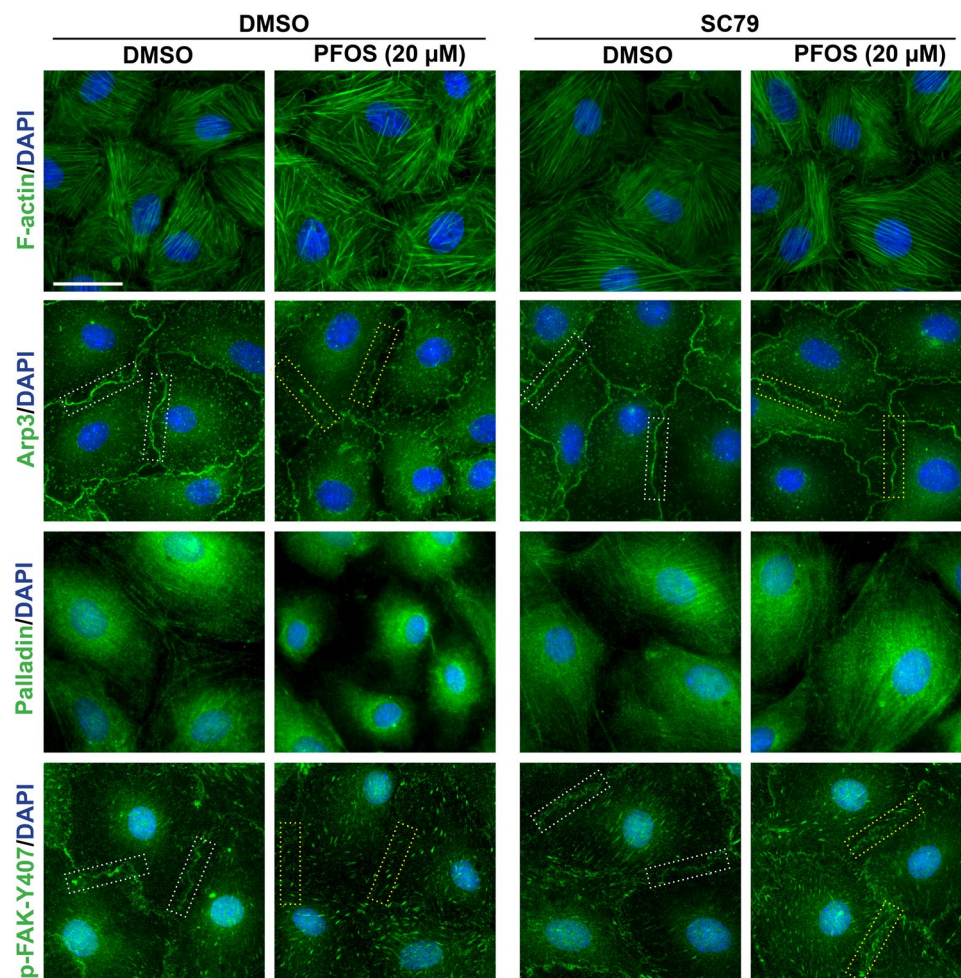


Figure 4. SC79 blocks PFOS-induced disorganization of actin microfilaments by maintaining proper spatial expression of actin regulatory proteins in Sertoli cells exposed to PFOS. Sertoli cells cultured at 0.03×10^6 cells/cm² for 3 days were pre-treated with 2 μ g/ml SC79 (5.5 μ M) for 30 min, and then cells were rinsed and treated with 20 μ M PFOS for 24 hr. Cells were then fixed and visualized by immunofluorescence microscopy. It was noted that Sertoli cells exposed to PFOS without pre-treatment with SC79 were grossly disorganized in which actin microfilaments were truncated, likely the result of changes in the spatial expression of Arp3 (a branched actin polymerization protein), palladin (an actin cross-linking and bundling protein) and p-FAK-Y407 (a BTB-associated signaling protein known to promote BTB integrity¹⁴). However, pretreatment of Sertoli cells with SC79 blocked the PFOS-induced disorganization of actin microfilaments, causing actin microfilaments to be organized similar to control cells even in the presence of PFOS for 24 hr. This blocking effect of SC79 on PFOS-induced Sertoli cell injury apparently was mediated by maintaining the proper spatial expression of Arp3, palladin and p-FAK-Y407 as noted in control cells. Distribution of the target proteins Arp3 and p-FAK-Y407 at the cell cortical zone was also quantified by measuring the fluorescence intensity at the Sertoli cell-cell interface (see dotted white rectangles in control cells vs. dotted yellow rectangles in PFOS-treated cells), which was the average of 4 measurements (i.e., fluorescence intensity) at two opposite ends of a Sertoli cell as annotated by the rectangles for each cell. About 70 randomly selected cells in each experiment were quantified with $n = 3$ independent experiments. Scale bar, 30 μ m, which applies to all other micrographs.

distribution across the cell cytosol as found in PFOS-treated cells alone (Fig. 4). These changes thus contributed to the re-organization of actin microfilaments so that SC79 rescued PFOS-mediated F-actin disorganization (Fig. 4).

PFOS dose-dependently mediates disorganization of microtubules (MTs). Treatment of Sertoli cells with PFOS was found to cause disorganization of MTs when α -tubulins (the building blocks of MTs) across the Sertoli cell cytosol were visualized by IF (Fig. 5). For instance, MTs no longer stretched across the cell cytosol as found in control cells (DMSO alone) but retracted closer to the cell nuclei when PFOS was used at 20 μ M. At 50 μ M, even more MTs were retracted to the cell nuclei (Fig. 5). Furthermore, detyrosinated α -tubulin (the stabilized form of MTs) no longer radiated from the Sertoli cell nuclei but retracted closer to nuclei when exposed to PFOS at 20 μ M, and considerably diminished more at 50 μ M (Fig. 5), illustrating the dose-dependent disruptive effects of PFOS, consistent with the IB findings shown in Fig. 1B. Interestingly, the +TIP (plus-end tracking protein) EB1 (known to stabilize MTs) also no longer stretched across the cell cytosol by forming aggregates along

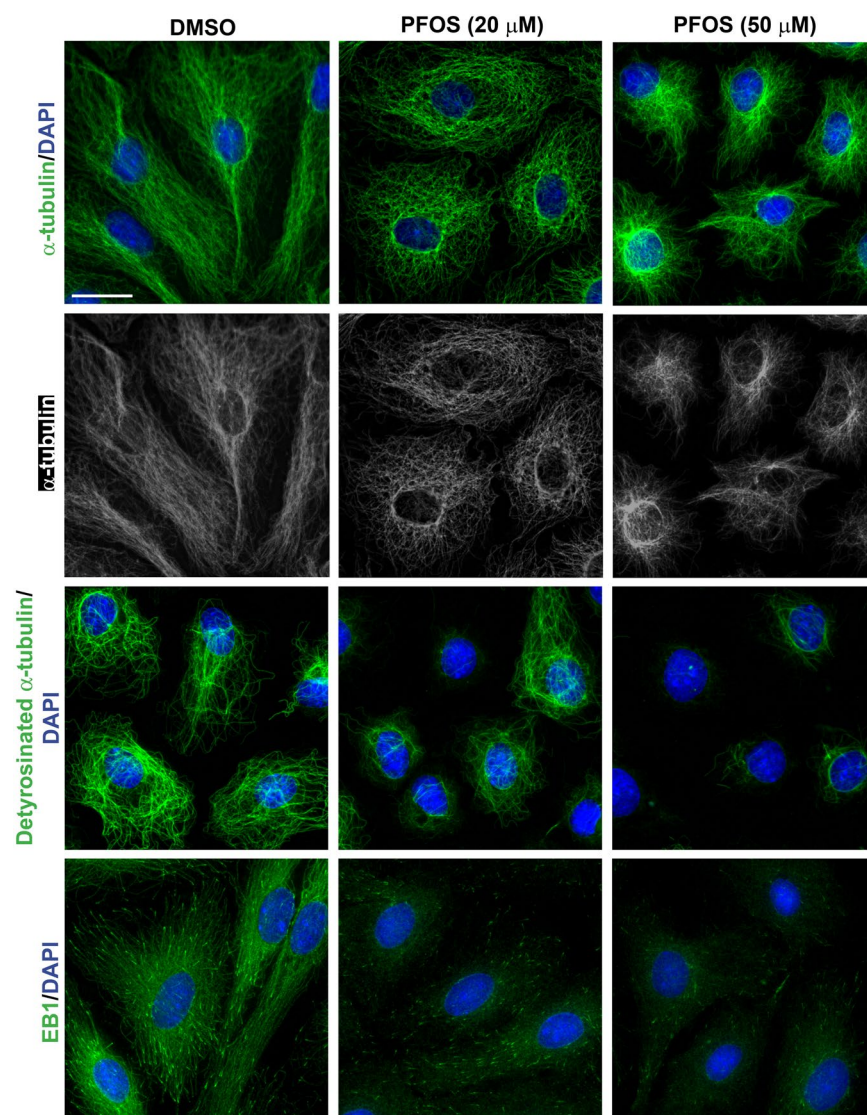


Figure 5. PFOS induces disorganization of microtubules (MTs) through its disruptive effects on the localization of α -tubulin and detyrosinated α -tubulin, and MT regulatory protein EB1. Sertoli cells cultured for 3 days at a density of 0.03×10^6 cells/cm². Cells were then treated with either 20 or 50 μ M PFOS for 24 hr. Thereafter, cells were fixed with ice-cold methanol and visualized by immunofluorescence microscopy. In control cells, α -tubulin, the building block of MTs, stretched across the entire Sertoli cell to support cell shape and served as tracks for intracellular transport and trafficking. Following PFOS treatment, there was a dose-dependent retraction of MTs across the cell cytosol wherein MTs no longer stretched across the cytosol but encircled the Sertoli cell nuclei instead. Detyrosinated α -tubulin, the stabilized form of MTs, was considerably diminished dose-dependently, consistent with findings shown in Fig. 1B. Interestingly, the spatial expression of EB1, a +TIP (plus-end tracking protein) was considerably disrupted since it no longer expressed prominently across the MTs as noted in control Sertoli cells, but apparently dispersed in the cell cytosol since the overall expression of EB1 was not shown to be down-regulated as noted by immunoblotting shown in Fig. 1B. Sertoli cell nuclei were visualized by DAPI. Scale bar, 30 μ m, which applies to all other micrographs.

the Sertoli cell MTs as noted in control (DMSO only) cells, but possibly dispersed singularly instead of aggregates so that the green fluorescence appeared to be weakened (Fig. 5) since no down-regulation of EB1 was noted following PFOS treatment in Sertoli cells (see Fig. 1B).

SC79 rescues PFOS-mediated disruption of MT organization through changes in detyrosinated α -tubulin and EB1 distribution. Treatment of Sertoli cells with SC79 also rescued PFOS-induced disruption of MT organization, in which MTs were found to stretch across the entire cell cytosol from cell nuclei instead of retracting from cell peripheries to form round-shaped cells in cells treated with PFOS (20 μ M) without SC79 (Fig. 6, top panel). This protective effect of SC79 appeared to be mediated by re-distributing detyrosinated α -tubulin (a stabilized form of MTs) in the Sertoli cell cytosol, so that detyrosinated α -tubulin that was retracted from the cell cytosol in PFOS-treated cells was found to radiate from the Sertoli cell nucleus and stretches further

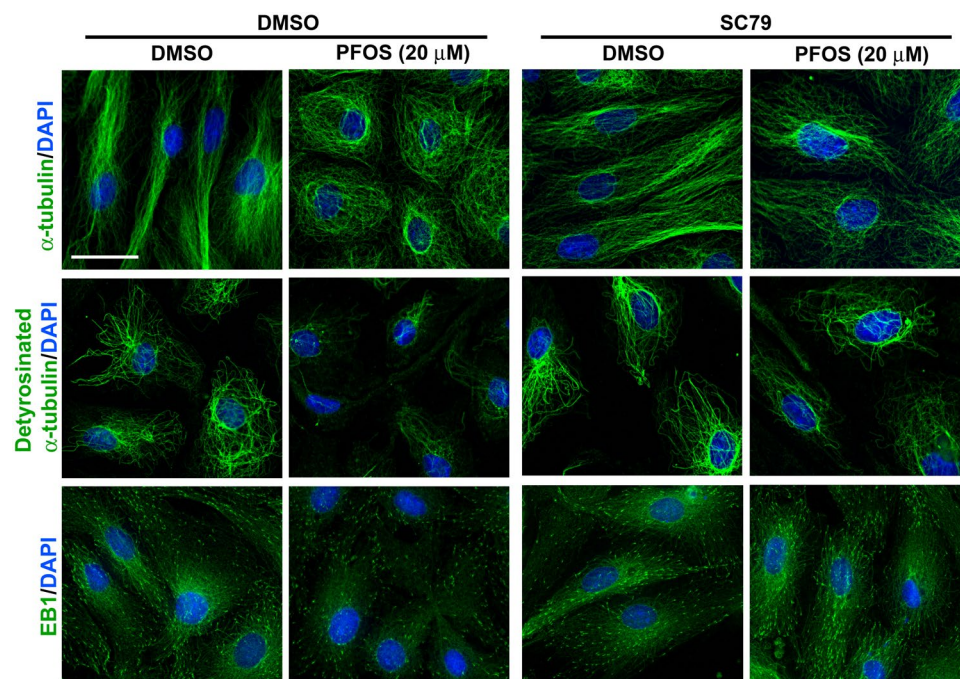


Figure 6. Akt activator SC79 blocks PFOS-mediated MT (e.g., α -tubulin and detyrosinated α -tubulin) disorganization by attenuating disruptive distribution of EB1. Sertoli cells cultured for 3 days at a density of 0.03×10^6 cells/cm². Cells were pre-treated with 2 μ g/ml SC79 (5.5 μ M) for 30 min, and then cells were rinsed and treated with PFOS at 20 μ M for 24 hr. Thereafter, cells were fixed with ice-cold methanol and visualized by immunofluorescence microscopy using corresponding antibodies (Table 1). Consistent with data shown in Fig. 5, PFOS induced disorganization of MTs by disrupting the organization of α -tubulin and detyrosinated α -tubulin across the Sertoli cell cytosol and also +TIP EB1. However, SC79 blocked the PFOS-mediated MT disorganization, possibly by attenuating disruptive distribution of EB1 in SC79 pre-treated cells. Sertoli cell nuclei were visualized by DAPI. Scale bar, 30 μ m, which applies to all other micrographs.

into the cell cytosol in SC79 pretreated cells (Fig. 6, **second panel**). Similarly, EB1, a +TIP, also stretched across the Sertoli cell cytosol following SC79 treatment, by preventing PFOS-induced mis-localization of EB1, in which EB1 formed aggregates along the MTs to induce MT stabilization in SC79-treated cells even with PFOS exposure, considerably different from Sertoli cells treated with PFOS alone (Fig. 6, **bottom panel**).

Discussion

Findings reported herein are consistent with other data in the literature that cytoskeletons in Sertoli cells, including both the F-actin and the microtubule (MT)-based cytoskeletons, are one of the targets of environmental toxicants (for reviews, see refs 40–45). Besides Sertoli cells isolated from rodent testes as noted herein, F-actin cytoskeleton in human Sertoli cells is also highly susceptible to environment toxicants, such as cadmium chloride (CdCl₂) and bisphenol A (BPA), which were shown to induce defragmentation of actin microfilaments in Sertoli cells, thereby perturbing the distribution of TJ proteins (e.g., ZO-1) and basal ES proteins (e.g., N-cadherin, β -catenin) at the Sertoli cell-cell interface⁴⁶. In this context, it is of interest to note that CdCl₂ remains widely used in the United States, such as manufacturing of batteries, and contaminating our environment through municipal waste incineration, plus an increase in human uptakes through contaminated water and food supplies including cigarette smoking; whereas BPA is found in many household items (e.g., utensils, plastics, food containers) (for BPA) (for reviews, see refs 34, 47). While the elimination half-life of BPA is short in humans (<2 hr), but cadmium has a half-life of >20 years so that considerable amount of toxic level of cadmium can build up in humans over time. Thus, the observation that human Sertoli cells are susceptible to these toxicants is of interest since these findings reproduce some of the earlier observations in studies using rodent Sertoli cells, illustrating F-actin organization is one of the targets of toxicants^{13, 48}. This unexpected disruption of the F-actin organization in Sertoli cells induced by toxicants such as PFOS as illustrated herein vs. cadmium and BPA shown earlier is of physiologically important, since these findings implicate that the BTB function is compromised in the testis *in vivo* following exposure to toxicants as noted earlier^{49–53}. This also explains earlier observations that the testis is highly vulnerable to toxicants (e.g., cadmium) as reported six decades ago^{54, 55}. Indeed, subsequent studies confirmed the BTB was compromised before changes in the permeability of the microvessels in the testis⁴⁹ when the kinetics of their disruption were assessed⁵⁶, illustrating while the BTB is one of the tightest blood-tissue barriers (for reviews, see refs 20, 57), it is highly susceptible to environmental toxicants when compared to other blood-tissue barriers such as the endothelial TJ-barrier. Studies in recent years have also cautioned a declining trend of semen quality and/or sperm counts in men is associated with an increase in environmental toxicant exposure^{58, 59}. Perhaps, this is due

to the readily disrupted BTB, this thus increases the bioavailability of the toxicant in the testis behind the BTB, exposing post-meiotic spermatids to the toxicant.

Thus, it is important to identify the signaling molecule(s) mediated by toxicants through which the BTB can be modulated. Akt (also known as PKB) is a Ser/Thr protein kinase composed of three closely related and widely expressed isoforms of Akt1, Akt2 and Akt3 found in virtually all mammalian cells (for reviews, see refs 60, 61) including Sertoli cells²¹. In fact, Akt/PKB is prominently expressed at the ES (a testis-specific actin-rich anchoring junction found at the Sertoli cell-cell interface at the BTB known as basal ES vs. the similar ultrastructure found at the Sertoli cell-spermatid interface known as apical ES in the adluminal (apical) compartment of the seminiferous epithelium (for reviews, see refs 62, 63)) in the adult rat testis²¹. As reported herein, Akt1/2 was shown to be a putative target of PFOS. First, treatment of Sertoli cells with an established functional TJ-barrier was found to perturb the barrier function, associated with a down-regulation on the expression of p-Akt1-T308, p-Akt1-S473, and p-Akt2-S474. Second, the use of SC79, an Akt activator, was found to restore the steady-state protein level of p-Akt1-T308 and p-Akt1-S473, but had no apparent effect on p-Akt2-S474. These findings thus illustrate that PFOS-induced p-Akt2-S474 down-regulation could not be rescued by SC79, and this down-regulation had no correlation with PFOS-induced Sertoli cell TJ-barrier disruption nor the underlying cytoskeletal disorganization. It is known that p-Akt1-T308 and p-Akt1-S473 are working in concert to modulate cellular functions⁶⁴. In fact, modification of Akt1 at T308 and S473 via phosphorylation has been established as the equivalent of Akt activation, illustrating these two sites are working in concert to modulate cellular function (for a review, see ref. 60). Thus, our findings that PFOS-induced p-Akt1-T308 and p-Akt1-S473 inactivation via their down-regulation, and a restoration of the leaky BTB by SC79 through an up-regulation of Akt1 at these two sites are consistent with the earlier reports^{60,65}. An interesting observation in this report is the finding that the use of SC79 was shown to induce re-organization of both F-actin- and MT-based cytoskeletons, making the PFOS-treated cells more similar to control cells, blocking the disruptive effects of PFOS on the organization of actin microfilaments and MTs. Since all the TJ- and basal ES-proteins are actin-based adhesion protein complexes, the re-establishment of the F-actin cytoskeleton thus provides the platform for re-distribution of these BTB-associated proteins so that the TJ-barrier function can be restored.

In this context, it is of interest to note that treatment of Sertoli cells with SC79 alone was found to up-regulate p-Akt1-T308 and p-Akt1-S473 (but not p-Akt2/S474), consistent with the concept that p-Akt1-T308 and p-Akt1-S473 are working together to regulate cell function⁶⁴, yet SC79 alone had no apparent effects on the Sertoli cell TJ-permeability barrier. These observations thus suggest that there are other proteins and/or signaling pathways involved in modulating the SC79-mediated rescue efforts following PFOS exposure regarding re-organization of the actin- and MT-based cytoskeletons. This notion is supported by studies demonstrating that overexpression of connexin 43 (Cx43, a gap junction protein highly expressed in the testis^{66,67} and a target of environmental toxicant⁶⁷) also intercepts the PFOS-induced BTB disruption and capable of rescuing PFOS-mediated F-actin disorganization³⁶. For instance, in the absence of PFOS, Cx43 *per se* that is known to maintain the Sertoli cell TJ-permeability barrier function^{68,69} might have conferred the TJ-barrier function to its maximal, thus, the presence of SC79, including the activation of p-Akt1-T308 and p-Akt1-S473 could no longer enhance the immunological barrier to make it "tighter". This possibility, however, must be carefully evaluated in future studies.

Earlier studies have shown that FAK, in particular p-FAK-Y407 is an important signaling molecule tightly involved in BTB integrity, playing a role in the organization of actin-based cytoskeleton in Sertoli cells^{14,70}. Studies in other mammalian cells have shown that FAK is the upstream signaling protein of Akt^{71,72}, and these two signaling proteins often work as close partners to modulate a number of cellular functions in particular tumorigenesis⁷³. In fact, we also report herein the use of SC79 could restore the spatial expression of p-FAK-Y407 in Sertoli cells disrupted by PFOS, suggesting that these two functional signaling kinases may indeed work together to modulate Sertoli cell BTB function. This possibility should be carefully evaluated in future studies.

In summary, we have demonstrated unequivocally that PFOS-mediated Sertoli cell BTB disruption can be rescued by the use of an Akt activator SC79, which apparently exerts its effects by re-establishing the underlying actin- and MT-based cytoskeletons, restoring the localization of BTB-associated adhesion protein complexes. This thus reveals the disrupted Sertoli cell TJ-permeability barrier induced by PFOS. These findings should be carefully evaluated and further expanded to include the use of human Sertoli cells to assess if an activation of p-Akt could rescue PFOS-mediated Sertoli cell injury since a recent report has shown that Sertoli cell injury induced by environmental toxicants is similar to Sertoli cells isolated from rodent testes⁴⁶. This additional study should be of important to therapeutically manage PFOS (or other environmental toxicants) induced testis injury and possibly infertility.

Materials and Methods

Animals and antibodies. Male Sprague-Dawley pups at 16–19 days of age, with a foster mother per 10 pups, were purchased from Charles River Laboratories (Kingston, NY). Animals were housed at the Rockefeller University Comparative Bioscience Center (CBC) with 10 pups and a foster mother per cage. All animals had free access to standard rat chow and water *ad libitum* under controlled temperature (22°C) and constant light-dark cycles (12 hr of light: 12 hr of darkness). These animals were maintained in accordance with the applicable portions of the Animal Welfare Act and the guidelines in the Department of Health and Human Services publication *Guide for the Care and Use of Laboratory Animals*. The use of rats for experiments reported herein was approved by the Rockefeller University Institutional Animal Care and Use Committee (IACUC) with Protocol Numbers 12–506 and 15–780-H. All methods and experimental protocols used for relevant studies reported herein, including the use of animals and primary Sertoli cell cultures were carried out in accordance with the relevant guidelines, including any relevant details, and approved by the Rockefeller University Laboratory Safety and Environmental Health, the Rockefeller University Institutional Biosafety Committee (IBC), and the Rockefeller

University Comparative Bioscience Center (CBC). These methods were also described in details in the sections below. Antibodies were obtained commercially and listed in Table 1.

Primary Sertoli cell cultures. Sertoli cells were isolated from the testes of 20-day-old rats as earlier described¹⁹. Cells were seeded on Matrigel (1:5–1:7, diluted in F12/DMEM; BD Biosciences, San Jose, CA)-coated Millipore Millicell HA bicameral units (12-mm diameter, 0.6-cm² effective surface area; 0.45-μm pore size; each unit was placed on a well of a 24-well dish containing 0.5 ml F12/DMEM in the apical and basal compartment), 6-well culture dishes (with each well contained 2 ml F12/DMEM to be used for lysate preparation) or coverslips (with each coverslip place on the well of a 12-well dish containing 1 ml F12/DMEM for immunofluorescence (IF) analysis) at densities of 1, 0.1 and $\sim 0.03\text{--}0.04 \times 10^6$ cells/cm², respectively. Sertoli cells were cultured in serum-free F12/DMEM (Thermo Fisher Scientific, Waltham, MA) supplemented with growth factors and gentamicin and incubated in a humidified atmosphere of 95% air/5% CO₂ (v/v) at 35 °C as described¹⁹. On day 2, Sertoli cells were subjected to a brief hypotonic treatment with 20 mM Tris (pH 7.4) for 2.5 min to lyse residual germ cells⁷⁴, and replaced with fresh medium containing antibiotics and supplements. These Sertoli cell cultures contained $\sim 98\%$ Sertoli cells, with negligible contaminations of Leydig cells, peritubular myoid cells, and/or germ cells when specific markers of these cell types were used to assess their contamination by either immunoblotting (IB) or RT-PCR as described⁷⁵. Sertoli cells cultured *in vitro* were shown to establish a functional TJ-permeability barrier with ultrastructures of TJs, basal ESs, gap junctions, and desmosomes that mimic the Sertoli cell BTB *in vivo* as described^{21,52}.

Treatment of Sertoli cells with perfluorooctanesulfonate (PFOS) and SC79.

Perfluorooctanesulfonate (PFOS) was obtained from Sigma-Aldrich (St. Louis, MO) and dissolved in DMSO at 100 mM. SC79 (2-amino-6-chloro- α -cyano-3-(ethoxycarbonyl)-4H-1-benzopyran-4-acetic acid ethyl ester, Mr 364.78), a specific Akt1/2 activator that binds to the pleckstrin homology (PH) domain of Akt, mimicking the binding of PtdIns(3,4,5)P₃ to induce Akt conformational change that enhances phosphorylation and activation at both the p-Akt1-T308 and p-Akt1-S473 sites³⁹, was purchased from Millipore (Billerica, MA). SC79 was freshly prepared at 25 μg/μl in DMSO. Sertoli cells cultured for 3 days was treated with DMSO (control) vs. 10, 20 or 50 μM PFOS for 24 hr. For the rescue experiments, Sertoli cells were pre-treated with 2 μg/ml SC79 (5.5 μM) for 30 min as earlier described³⁹, and then cells were rinsed and treated with PFOS (20 μM for IF; 50 μM for IB) for 24 hr. The same amount of DMSO was used in controls. The approach of pretreating cells with SC79 to examine its effects on Akt signaling was similar to earlier reports^{39,76}. However, in the experiments where the effects of SC79 to attenuate PFOS-mediated Sertoli cell TJ-barrier disruption were investigated, besides pre-treating cells with SC79 for 30 min, SC79 was also included during treatment of cells with PFOS for 24 hr. The selected concentrations of PFOS used in our experiments were based on earlier studies^{13,23,77}, and were earlier shown to have no detectable cytotoxicity in Sertoli cells¹³. The concentration of SC79 used in our studies was similar to earlier studies on mammalian cells and tissues both *in vitro* and *in vivo* without cytotoxicity^{39,78}.

Lysate preparation and immunoblotting (IB). Protein lysates from primary Sertoli cells were obtained using IP lysis buffer [50 mM Tris, 0.15 M NaCl, 1% NP-40, 2 mM EGTA, and 10% glycerol (v/v), pH 7.4 at 22 °C] supplemented with protease phosphatase inhibitor mixture (Sigma-Aldrich) and phosphatase inhibitor mixture II (Sigma-Aldrich). Protein concentration was determined using a DC Protein Assay Kit from Bio-Rad (Hercules, CA). About 25–40 μg protein was used from each sample for immunoblotting. In short, equal amount of protein lysate from all samples within an experiment were resolved by SDS-PAGE and transferred onto nitrocellulose membrane (Bio-Rad) for immunoblot analysis using the corresponding primary and secondary antibody for a target protein (Table 1). Each target protein was visualized by enhanced chemiluminescence using a kit prepared in our laboratory as described⁷⁹. Digital images were acquired and quantified using a Fujifilm LAS-4000 mini-Luminiscent Image Analyzer and Multi Gauge software package (Version 3.1) from Fujifilm Corp (Valhalla, NY) as earlier reported³⁵. Due to space limitation to display multiple immunoblots, blots were cropped to illustrate only the target proteins to compare changes between treatment and control groups, and full-length blots for blots reported in Fig. 1B and Fig. 3A are shown in Figures S4 and S5, respectively, in Supplementary Information.

Immunofluorescence (IF) analysis. IF was performed using Sertoli cells cultured on coverslips at a density of $\sim 0.03\text{--}0.04 \times 10^6$ cells/cm². Sertoli cells were fixed in 4% PFA in PBS (10 mM sodium phosphate, 0.15 M NaCl, pH 7.4 at 22 °C) or ice-cold methanol, permeabilized with 0.1% Triton X-100 in PBS, and subsequently blocked with 1% BSA in PBS. Cells were then incubated with the corresponding primary antibodies (Table 1) at 4 °C overnight, to be followed by Alexa Fluor 488 (green) secondary antibodies (Thermo Fisher Scientific) for 1 hr. To visualize F-actin, sections and/or cells were incubated with FITC-conjugated phalloidin (Thermo Fisher Scientific) at 1:50 dilution for 1 hr. Cells on microscopic slides were mounted in Prolong Gold Antifade reagent with 4', 6-diamidino-2-phenylindole (DAPI, Life Technologies) to visualize cell nuclei. Fluorescence images were examined and acquired using a Nikon Eclipse 90i Fluorescence Microscope system equipped with a Nikon Ds-Qi1Mc and a Nikon DS-Fi1 digital cameras, using the Nikon NIS Elements Imaging Software (Nikon Instruments, Inc). Image files were then analyzed using Photoshop in Adobe Creative Suite (Version 3.0; San Jose, CA) for image overlay to assess protein co-localization. All Sertoli cells within an experimental group were processed simultaneously in a single experimental session to eliminate interexperimental variations and each experiment was repeated at least 3 times. To assess changes in protein expression and/or distribution following treatment with DMSO by immunofluorescence microscopy, fluorescence intensity at the Sertoli cell-cell interface

of a target protein in control vs. treatment group (at two opposite ends of adjacent cells, i.e., 4 measurements, to obtain an average which was the mean fluorescence intensity) in *in vitro* experiments was quantified using ImageJ 1.45 software (NIH, Bethesda, MD; <http://rsbweb.nih.gov/ij/>). For changes in protein localization near the Sertoli cell cortical zone, the distribution of fluorescence signals at the cell-cell interface was measured at the two opposite ends (i.e., 4 measurements) of the Sertoli cell nucleus, which was then averaged to obtain the mean width. At least 200 cells were randomly selected and examined in control vs. experimental groups with $n = 3$ experiments (i.e., ~70 randomly selected cells per experiment).

Monitoring the Sertoli cell TJ-permeability barrier function *in vitro*. Sertoli cells were plated on Matrigel (1:5)-coated bicameral units at 1×10^6 cells/cm². Bicameral units were then placed in 24-well plates with 0.5 ml F12/DMEM each in the apical and basal compartment. To assess the TJ-permeability barrier, both the PFOS and the control (DMSO) group contained triplicate bicameral units, and TER (transepithelial electrical resistance) across the cell epithelium was recorded daily. It is noted that TER monitored the ability of the Sertoli cell epithelium on the bicameral unit to resist conductivity of an electrical current that was sent across the electrodes of the Millipore Millicell ERS system as described¹⁹. Blanks contained Matrigel-coated bicameral units without Sertoli cells. TER experiments were repeated at least 3 times using different batches of Sertoli cells and yielded similar results.

Statistical analysis. For studies using Sertoli cell cultures, triplicate coverslips, wells, or bicameral units were used for each experiment including treatment and control groups. Each data point (or bar graph) is a mean \pm SD of $n = 3$ to 5 experiments. Statistical analysis was performed by one-way ANOVA followed by Dunnett's test or nonparametric Mann-Whitney *U* test. In selected experiments, Student's *t*-test was used for paired comparisons. Statistical analysis was performed using the GB-STAT software package (Version 7.0; Dynamic Microsystems, Silver Spring, MD). Mann-Whitney *U* test was performed using GraphPad Prism (Version 5.0, GraphPad Software, La Jolla, CA). $P < 0.05$ or smaller was considered statistically significant.

References

- Olsen, G. W., Butenhoff, J. L. & Zobel, L. R. Perfluoroalkyl chemicals and human fetal development: an epidemiologic review with clinical and toxicological perspectives. *Reprod Toxicol* **27**, 212–230, doi:10.1016/j.reprotox.2009.02.001 (2009).
- Bach, C. C. *et al.* Perfluoroalkyl and polyfluoroalkyl substances and human fetal growth: a systematic review. *Crit Rev Toxicol* **45**, 53–67, doi:10.3109/10408444.2014.952400 (2015).
- Lau, C., Butenhoff, J. L. & Rogers, J. M. The developmental toxicity of perfluoroalkyl acids and their derivatives. *Toxicol Appl Pharmacol* **198**, 231–241, doi:10.1016/j.taap.2003.11.031 (2004).
- Taxvig, C., Rosenmai, A. K. & Vinggaard, A. M. Polyfluorinated alkyl phosphate ester surfactants - current knowledge and knowledge gaps. *Basic Clin Pharmacol Toxicol* **115**, 41–44, doi:10.1111/bcpt.2014.115.issue-1 (2014).
- Chang, E. T. *et al.* A critical review of perfluorooctanoate and perfluorooctanesulfonate exposure and cancer risk in humans. *Crit Rev Toxicol* **44** (Suppl 1), 1–81, doi:10.3109/10408444.2014.905767 (2014).
- Itoh, S. *et al.* Association of perfluoroalkyl substances exposure in utero with reproductive hormone levels in cord blood in the Hokkaido Study on Environment and Children's Health. *Environ Int* **94**, 51–59, doi:10.1016/j.envint.2016.05.011 (2016).
- Olsen, G. W. *et al.* Half-life of serum elimination of perfluorooctanesulfonate, perfluorohexanesulfonate, and perfluorooctanoate in retired fluorocarbon production workers. *Environ Health Perspect* **115**, 1298–1305, doi:10.1289/ehp.10009 (2007).
- Fromme, H., Tittlemier, S. A., Volk, W., Wilhelm, M. & Twardella, D. Perfluorinated compounds - exposure assessment for the general population in Western countries. *Int J Hyg Environ Health* **212**, 239–270, doi:10.1016/j.ijheh.2008.04.007 (2009).
- Dankers, A. C. *et al.* Endocrine disruptors differentially target ATP-binding cassette transporters in the blood-testis barrier and affect Leydig cell testosterone secretion in vitro. *Toxicol Sci* **136**, 382–391, doi:10.1093/toxsci/kft198 (2013).
- Zhang, J., Liang, J., Zhu, H., Li, C. & Wu, Q. PFOS and PCB 153 have direct adverse effects on neonatal testis modeled using a coculture of primary gonocyte and Sertoli cells. *Environ Toxicol* **28**, 322–331, doi:10.1002/tox.v28.6 (2013).
- Wan, H. T. *et al.* Testicular signaling is the potential target of perfluorooctanesulfonate-mediated subfertility in male mice. *Biol Reprod* **84**, 1016–1023, doi:10.1095/biolreprod.110.089219 (2011).
- Zhao, B. *et al.* Inhibition of human and rat 3 β -hydroxysteroid dehydrogenase and 17 β -hydroxysteroid dehydrogenase 3 activities by perfluoroalkylated substances. *Chem Biol Interact* **188**, 38–43, doi:10.1016/j.cbi.2010.07.001 (2010).
- Wan, H. T., Mruk, D. D., Wong, C. K. C. & Cheng, C. Y. Perfluorooctanesulfonate (PFOS) perturbs male rat Sertoli cell blood-testis barrier function by affecting F-actin organization via p-FAK-Tyr⁴⁰⁷ - an *in vitro* study. *Endocrinology* **155**, 249–262, doi:10.1210/en.2013-1657 (2014).
- Lie, P. P. Y. *et al.* Focal adhesion kinase-Tyr⁴⁰⁷ and -Tyr³⁹⁷ exhibit antagonistic effects on blood-testis barrier dynamics in the rat. *Proc Natl Acad Sci USA* **109**, 12562–12567, doi:10.1073/pnas.1202316109 (2012).
- Mok, K. W., Chen, H., Lee, W. M. & Cheng, C. Y. rpS6 regulates blood-testis barrier dynamics through Arp3-mediated actin microfilament organization in rat Sertoli cells. An *in vitro* study. *Endocrinology* **156**, 1900–1913, doi:10.1210/en.2014-1791 (2015).
- Mok, K. W., Mruk, D. D. & Cheng, C. Y. rpS6 regulates blood-testis barrier dynamics through Akt-mediated effects on MMP-9. *J Cell Sci* **127**, 4870–4882, doi:10.1242/jcs.152231 (2014).
- Byun, H. J. *et al.* Anti-angiogenic effects of thioridazine involving the FAK-mTOR pathway. *Microvasc Res* **84**, 227–234, doi:10.1016/j.mvr.2012.09.006 (2012).
- Tong, B. *et al.* Gleditsioside B, a triterpene saponin isolated from the anomalous fruits of *Gleditsia sinensis* Lam., abrogates bFGF-induced endothelial cell migration through preventing the activation of MMP-2 and FAK via inhibiting ERK and PI3K/AKT signaling pathways. *Vascul Pharmacol* **58**, 118–126, doi:10.1016/j.vph.2012.09.006 (2013).
- Mruk, D. D. & Cheng, C. Y. An *in vitro* system to study Sertoli cell blood-testis barrier dynamics. *Methods Mol Biol* **763**, 237–252, doi:10.1007/978-1-61779-191-8_16 (2011).
- Cheng, C. Y. & Mruk, D. D. The blood-testis barrier and its implication in male contraception. *Pharmacol Rev* **64**, 16–64, doi:10.1124/pr.110.002790 (2012).
- Siu, M. K. Y., Wong, C. H., Lee, W. M. & Cheng, C. Y. Sertoli-germ cell anchoring junction dynamics in the testis are regulated by an interplay of lipid and protein kinases. *J Biol Chem* **280**, 25029–25047, doi:10.1074/jbc.M501049200 (2005).
- Lee, N. P. Y. & Cheng, C. Y. Regulation of Sertoli cell tight junction dynamics in the rat testis via the nitric oxide synthase/soluble guanylate cyclase/3',5'-cyclic guanosine monophosphate/protein kinase G signaling pathway: an *in vitro* study. *Endocrinology* **144**, 3114–3129, doi:10.1210/en.2002-0167 (2003).

23. Qiu, L. *et al.* Sertoli cell is a potential target for perfluorooctane sulfonate-induced reproductive dysfunction in male mice. *Toxicol Sci* **135**, 229–240, doi:10.1093/toxsci/kft129 (2013).
24. Nicholls, P. K., Harrison, C. A., Gilchrist, R. B., Farnworth, P. G. & Stanton, P. G. Growth differentiation factor 9 is a germ cell regulator of Sertoli cell function. *Endocrinology* **150**, 2481–2490, doi:10.1210/en.2008-1048 (2009).
25. Janeczek, A., Jakubowiak, A. & Steinberger, A. Effect of cadmium chloride on transepithelial electrical resistance of Sertoli cell monolayers in two-compartment cultures - a new model for toxicological investigations of the "blood-testis" barrier *in vitro*. *Toxicol Appl Pharmacol* **112**, 51–57, doi:10.1016/0041-008X(92)90278-Z (1992).
26. Byers, S., Hadley, M. A., Djakiew, D. & Dym, M. Growth and characterization of epididymal epithelial cells and Sertoli cells in dual environment culture chambers. *J Androl* **7**, 59–68, doi:10.1002/j.1939-4640.1986.tb00871.x (1986).
27. Kaitu'u-Lino, T. J., Sluka, P., Foo, C. F. & Stanton, P. G. Claudin-11 expression and localisation is regulated by androgens in rat Sertoli cells *in vitro*. *Reproduction* **133**, 1169–1179, doi:10.1530/REP-06-0385 (2007).
28. Du, M. *et al.* A novel subcellular machine contributes to basal junction remodeling in the seminiferous epithelium. *Biol Reprod* **88**, 60, doi:10.1095/biolreprod.112.104851 (2013).
29. Grima, J., Pineau, C., Bardin, C. W. & Cheng, C. Y. Rat Sertoli cell clusterin, α_2 -macroglobulin, and testins: biosynthesis and differential regulation by germ cells. *Mol Cell Endocrinol* **89**, 127–140, doi:10.1016/0303-7207(92)90219-V (1992).
30. Lui, W. Y., Wong, C. H., Mruk, D. D. & Cheng, C. Y. TGF- β 3 regulates the blood-testis barrier dynamics via the p38 mitogen activated protein (MAP) kinase pathway: an *in vivo* study. *Endocrinology* **144**, 1139–1142, doi:10.1210/en.2002-0211 (2003).
31. Su, L., Mruk, D. D., Lie, P. P. Y., Silvestrini, B. & Cheng, C. Y. A peptide derived from laminin-g3 reversibly impairs spermatogenesis in rats. *Nat Commun* **3**, 1185, doi:1110.1038/ncomms2171 (2012).
32. Gao, Y., Mruk, D. D., Lui, W. Y., Lee, W. M. & Cheng, C. Y. F5-peptide induces aspermatogenesis by disrupting organization of actin- and microtubule-based cytoskeletons in the testis. *Oncotarget* **7**, 64203–64220, doi:10.18632/oncotarget.11887 (2016).
33. Haverfield, J. T. *et al.* Differential permeability of the blood-testis barrier during reinitiation of spermatogenesis in adult male rats. *Endocrinology* **155**, 1131–1144, doi:10.1210/en.2013-1878 (2014).
34. Wan, H. T., Mruk, D. D., Wong, C. K. C. & Cheng, C. Y. Targeting testis-specific proteins to inhibit spermatogenesis - lesion from endocrine disrupting chemicals. *Expert Opin Ther Targets* **17**, 839–855, doi:10.1517/14728222.2013.791679 (2013).
35. Gao, Y., Lui, W. Y., Lee, W. M. & Cheng, C. Y. Polarity protein Crumbs homolog-3 (CRB3) regulates ectoplasmic specialization dynamics through its action on F-actin organization in Sertoli cells. *Scientific reports* **6**, 28589, doi:10.1038/srep28589 (2016).
36. Li, N. *et al.* Rescue of perfluorooctanesulfonate (PFOS)-mediated Sertoli cell injury by overexpression of gap junction protein connexin 43. *Scientific reports* **6**, 29667, doi:10.1038/srep29667 (2016).
37. Jiang, K. & Akhmanova, A. Microtubule tip-interacting proteins: a view from both ends. *Curr Opin Cell Biol* **23**, 94–101, doi:10.1016/j.ceb.2010.08.008 (2011).
38. Kreis, T. E. Microtubules containing detyrosinated tubulin are less dynamic. *EMBO J* **6**, 2597–2606 (1987).
39. Jo, H. *et al.* Small molecule-induced cytosolic activation of protein kinase Akt rescues ischemia-elicited neuronal death. *Proc Natl Acad Sci USA* **109**, 10581–10586, doi:10.1073/pnas.1202810109 (2012).
40. Boekelheide, K. *et al.* 2,5-Hexanedione-induced testicular injury. *Annu Rev Pharmacol Toxicol* **43**, 125–147, doi:10.1146/annurev.pharmtox.43.100901.135930 (2003).
41. Boekelheide, K. Mechanisms of toxic damage to spermatogenesis. *J Natl Cancer Inst Monogr* **34**, 6–8, doi:10.1093/jncimonographs/lgi006 (2005).
42. Boekelheide, K., Neely, M. D. & Sioussat, T. M. The Sertoli cell cytoskeleton: a target for toxicant-induced germ cell loss. *Toxicol Appl Pharmacol* **101**, 373–389, doi:10.1016/0041-008X(89)90188-9 (1989).
43. Li, N., Mruk, D. D., Lee, W. M., Wong, C. K. C. & Cheng, C. Y. Is toxicant-induced Sertoli cell injury *in vitro* a useful model to study molecular mechanisms in spermatogenesis? *Semin Cell Dev Biol* **59**, 141–156, doi:10.1016/j.semcdb.2016.01.003 (2016).
44. Cheng, C. Y. Toxicants target cell junctions in the testis - insights from the indazole-carboxylic acid model. *Spermatogenesis* **4**, e981485, doi:10.4161/21565562.2014.9814895 (2014).
45. Gao, Y., Mruk, D. D. & Cheng, C. Y. Sertoli cells are the target of environmental toxicants in the testis - a mechanistic and therapeutic insight. *Expert Opin Ther Targets* **19**, 1073–1090, doi:10.1517/14728222.2015.1039513 (2015).
46. Xiao, X. *et al.* Environmental toxicants perturb human Sertoli cell adhesive function via changes in F-actin organization mediated by actin regulatory proteins. *Hum Reprod* **29**, 1279–1291, doi:10.1093/humrep/deu011 (2014).
47. Siu, E. R., Mruk, D. D., Porto, C. S. & Cheng, C. Y. Cadmium-induced testicular injury. *Toxicol Appl Pharmacol* **238**, 240–249, doi:10.1016/j.taap.2009.01.028 (2009).
48. Siu, E. R. *et al.* An occludin-focal adhesion kinase protein complex at the blood-testis barrier: a study using the cadmium model. *Endocrinology* **150**, 3336–3344, doi:10.1210/en.2008-1741 (2009).
49. Setchell, B. P. & Waites, G. M. H. Changes in the permeability of the testicular capillaries and of the "blood-testis barrier" after injection of cadmium chloride in the rat. *J Endocrinol* **47**, 81–86, doi:10.1677/joe.0.0470081 (1970).
50. Hew, K. W., Heath, G. L., Jiwa, A. H. & Welsh, M. J. Cadmium *in vivo* causes disruption of tight junction-associated microfilaments in rat Sertoli cells. *Biol Reprod* **49**, 840–849, doi:10.1095/biolreprod49.4.840 (1993).
51. Wong, C. H., Mruk, D. D., Lui, W. Y. & Cheng, C. Y. Regulation of blood-testis barrier dynamics: an *in vivo* study. *J Cell Sci* **117**, 783–798, doi:10.1242/jcs.00900 (2004).
52. Li, M. W. M., Mruk, D. D., Lee, W. M. & Cheng, C. Y. Disruption of the blood-testis barrier integrity by bisphenol A *in vitro*: Is this a suitable model for studying blood-testis barrier dynamics? *Int J Biochem Cell Biol* **41**, 2302–2314, doi:10.1016/j.biocel.2009.05.016 (2009).
53. Wiebe, J., Kowalik, A., Gallardi, R., Egeler, O. & Clubb, B. Glycerol disrupts tight junction-associated actin microfilaments, occludin, and microtubules in Sertoli cells. *J Androl* **21**, 625–635 (2000).
54. Parizek, J. & Zahor, Z. Effect of cadmium salts on testicular tissue. *Nature* **177**, 1036–1037, doi:10.1038/1771036a0 (1956).
55. Parizek, J. Sterilization of the male by cadmium salts. *J Reprod Fertil* **1**, 294–309, doi:10.1530/jrf.0.0010294 (1960).
56. Wong, C. H., Mruk, D. D., Siu, M. K. Y. & Cheng, C. Y. Blood-testis barrier dynamics are regulated by α_2 -macroglobulin via the c-Jun N-terminal protein kinase pathway. *Endocrinology* **146**, 1893–1908, doi:10.1210/en.2004-1464 (2005).
57. Pelletier, R. M. The blood-testis barrier: the junctional permeability, the proteins and the lipids. *Prog Histochem Cytochem* **46**, 49–127, doi:10.1016/j.proghi.2011.05.001 (2011).
58. Rolland, M., Le Moal, J., Wagner, V., Royere, D. & De Mouzon, J. Decline in semen concentration and morphology in a sample of 26,609 men close to general population between 1989 and 2005 in France. *Hum Reprod* **28**, 462–470, doi:10.1093/humrep/des415 (2013).
59. Toft, G. *et al.* Exposure to perfluorinated compounds and human semen quality in Arctic and European populations. *Human Reprod* **27**, 2532–2540, doi:10.1093/humrep/des185 (2012).
60. Risso, G., Blaustein, M., Pozzi, B., Mammi, P. & Srebrow, A. Akt/PKB: one kinase, many modifications. *Biochem J* **468**, 203–214, doi:10.1042/BJ20150041 (2015).
61. Tokar, A. & Marmiroli, S. Signaling specificity in the Akt pathway in biology and disease. *Advances in biological regulation* **55**, 28–38, doi:10.1016/j.jbior.2014.04.001 (2014).
62. Vogl, A. W., Vaid, K. S. & Guttman, J. A. The Sertoli cell cytoskeleton. *Adv Exp Med Biol* **636**, 186–211, doi:10.1007/978-0-387-09597-4_11 (2008).

63. Cheng, C. Y. & Mruk, D. D. A local autocrine axis in the testes that regulates spermatogenesis. *Nature Rev Endocrinol* **6**, 380–395, doi:10.1038/nrendo.2010.71 (2010).
64. Ma, P. C. *et al.* Downstream signalling and specific inhibition of c-MET/HGF pathway in small cell lung cancer: implications for tumour invasions. *Br J Cancer* **97**, 368–377, doi:10.1038/sj.bjc.6603884 (2007).
65. Hers, I., Vincent, E. & Tavaré, J. M. Akt signalling in health and disease. *Cell Signal* **23**, 1515–1527, doi:10.1016/j.cellsig.2011.05.004 (2011).
66. Li, M. W. M., Mruk, D. D. & Cheng, C. Y. Gap junctions and blood-tissue barriers. *Adv Exp Med Biol* **763**, 260–280 (2012).
67. Pointis, G., Gilleron, J., Carrette, D. & Segretain, D. Testicular connexin 43, a precocious molecular target for the effect of environmental toxicants on male fertility. *Spermatogenesis* **1**, 303–317, doi:10.4161/spmg.1.4.18392 (2011).
68. Li, M. W. M., Mruk, D. D., Lee, W. M. & Cheng, C. Y. Connexin 43 is critical to maintain the homeostasis of blood-testis barrier via its effects on tight junction reassembly. *Proc Natl Acad Sci USA* **107**, 17998–18003, doi:10.1073/pnas.1007047107 (2010).
69. Li, M. W. M., Mruk, D. D., Lee, W. M. & Cheng, C. Y. Connexin 43 and plakophilin-2 as a protein complex that regulates blood-testis barrier dynamics. *Proc Natl Acad Sci USA* **106**, 10213–10218, doi:10.1073/pnas.0901700106 (2009).
70. Li, S. Y., Mruk, D. D. & Cheng, C. Y. Focal adhesion kinase is a regulator of F-actin dynamics: New insights from studies in the testis. *Spermatogenesis* **3**, e25385, doi:10.4161/spmg.25385 (2013).
71. Sonoda, Y., Watanabe, S., Matsumoto, Y., Aizu-Yokota, E. & Kasahara, T. FAK is the upstream signal protein of the phosphatidylinositol 3-kinase-Akt survival pathway in hydrogen peroxide-induced apoptosis of a human glioblastoma cell line. *J Biol Chem* **274**, 10566–10570, doi:10.1074/jbc.M313265200 (2004).
72. Xia, H., Nho, R. S., Kahm, J., Kleidon, J. & Henke, C. A. Focal adhesion kinase is upstream of phosphatidylinositol 3-kinase/Akt in regulating fibroblast survival in response to contraction of type I collagen matrices via a beta 1 integrin viability signaling pathway. *J Biol Chem* **279**, 33024–33034, doi:10.1074/jbc.M313265200 (2004).
73. Wang, S. & Basson, M. D. Protein kinase B/AKT and focal adhesion kinase: two close signaling partners in cancer. *Anti-Cancer Agents Med Chem* **11**, 993–1002, doi:10.2174/187152011797927661 (2011).
74. Galdieri, M., Ziparo, E., Palombi, F., Russo, M. A. & Stefanini, M. Pure Sertoli cell cultures: a new model for the study of somatic-germ cell interactions. *J Androl* **2**, 249–254, doi:10.1002/j.1939-4640.1981.tb00625.x (1981).
75. Lee, N. P. Y., Mruk, D. D., Conway, A. M. & Cheng, C. Y. Zyxin, axin, and Wiskott-Aldrich syndrome protein are adaptors that link the cadherin/catenin protein complex to the cytoskeleton at adherens junctions in the seminiferous epithelium of the rat testis. *J Androl* **25**, 200–215, doi:10.1002/j.1939-4640.2004.tb02780.x (2004).
76. Gong, Y. *et al.* SC79 protects retinal pigment epithelium cells from UV radiation via activating Akt-Nrf2 signaling. *Oncotarget* **7**, 60123–60132, doi:10.18632/oncotarget.11164 (2016).
77. Wan, H. T., Zhao, Y. G., Leung, P. Y. & Wong, C. K. C. Perinatal exposure to perfluorooctane sulfonate affects glucose metabolism in adult offspring. *PLoS One* **9**, e87137, doi:10.1371/journal.pone.0087137 (2014).
78. Zhang, D. *et al.* Akt specific activator SC79 protects against early brain injury following subarachnoid hemorrhage. *ACS chemical neuroscience* **7**, 710–718, doi:10.1021/acschemneuro.5b00306 (2016).
79. Mruk, D. D. & Cheng, C. Y. Enhanced chemiluminescence (ECL) for routine immunoblotting. An inexpensive alternative to commercially available kits. *Spermatogenesis* **1**, 121–122, doi:10.4161/spmg.1.2.16606 (2011).

Acknowledgements

We wish to thank Dr. Ben Margolis and Dr. Shuling Fan who kindly provided us with some anti-CR3 antibody to validate some experiments in this report. This work was supported by grants from the National Institutes of Health (R01 HD056034 to C.Y.C.; U54 HD029990 Project 5 to C.Y.C.); National Natural Science Foundation of China (NSFC) (31371176 to X.X.), Qianjiang Talents Program (QJD1502029 to X.X.), Zhejiang Province Funding (Science Technology Department, 2016F10010 to X.X.); Hong Kong Research Grants Council (RGC) General Research Fund (GRF) (774213 and 17100816 to W.Y.L.; 771513 to W.M.L.), NSFC/RGC Joint Research Scheme (N_HKU 717/12 to W.M.L.), and University of Hong Kong CRG Seed Funding (to W.M.L.).

Author Contributions

C.Y.C., Y.G. and H.C. designed research; Y.G., H.C. and C.Y.C. performed research; X.X., W.Y.L., W.M.L., D.D.M. and C.Y.C. contributed new reagents/analytic tools; Y.G., H.C. and C.Y.C. analyzed data; Y.G. and C.Y.C. wrote the paper; Y.G., H.C. and C.Y.C. prepared all figures. All authors reviewed the manuscript.

Additional Information

Supplementary information accompanies this paper at doi:10.1038/s41598-017-01016-8

Competing Interests: The authors declare that they have no competing interests.

Change History: A correction to this article has been published and is linked from the HTML version of this paper. The error has been fixed in the paper.

Publisher's note: Springer Nature remains neutral with regard to jurisdictional claims in published maps and institutional affiliations.



Open Access This article is licensed under a Creative Commons Attribution 4.0 International License, which permits use, sharing, adaptation, distribution and reproduction in any medium or format, as long as you give appropriate credit to the original author(s) and the source, provide a link to the Creative Commons license, and indicate if changes were made. The images or other third party material in this article are included in the article's Creative Commons license, unless indicated otherwise in a credit line to the material. If material is not included in the article's Creative Commons license and your intended use is not permitted by statutory regulation or exceeds the permitted use, you will need to obtain permission directly from the copyright holder. To view a copy of this license, visit <http://creativecommons.org/licenses/by/4.0/>.

© The Author(s) 2017